Geotextiles and Geomembranes 43 (2015) 283–292

Contents lists available at ScienceDirect

Geotextiles and Geomembranes

journal homepage: www.elsevier.com/locate/geotexmem

Field study of treatment for expansive soil/rock channel slope with soilbags

Sihong Liu [a], Yang Lu [a,*], Liping Weng [b], Fuqing Bai [c]

[a] College of Water Conservancy and Hydropower, Hohai University, Xi-Kang Road 1#, Nanjing 210098, China
[b] Business School of Hohai University, Xi-Kang Road 1#, Nanjing 210098, China
[c] Powerchina Huangdong Engineering Corporation Limited, Chao-Wang Road 22#, Hangzhou 310014, China

ARTICLE INFO

Article history:
Received 9 January 2015
Received in revised form
9 April 2015
Accepted 12 April 2015
Available online

Keywords:
Geosynthetics
Soilbags
Expansive soil/rock slope
Rainfall
Water content
Earth pressure

ABSTRACT

A full-scale field test in the South-to-North Water Transfer Project (SNWTP) in China was conducted on a 60 m long expansive soil/rock channel slope reinforced with soilbags. The field test involved the construction of the soilbags, the rising and falling of the channel water level as well as the natural and artificial rainfalls. During the testing period, in-situ monitoring of water contents, earth pressures and lateral displacements was conducted. It was found that: 1) the water content of the expansive soil/rock slope changed slightly with the rainfalls and other environmental factors after the reinforcement with soilbags; 2) the earth pressure measured under the soilbags layer was close to its overburden pressure with no swelling pressure of the expansive soil contained in the bags; and 3) the lateral displacement of the expansive soil/rock channel slope mainly occurred before the construction of the soilbags layer and tended to be stable after the completion of the soilbags layer. The monitored results suggested the effectiveness of soilbags to prevent moisture migration, mitigate the swelling potential and enhance the slope stability.

1. Introduction

Expansive or swelling soil is a highly plastic soil that typically contains montmorillonite and other active clay minerals. It exhibits significant swelling and shrinking upon wetting and drying (Dif and Bluemel, 1991; Zemenu et al., 2009; Ito and Azam, 2010), and usually an abundance of cracks and fissures develop in the upper part of the soil profile (Morris et al., 1992; Shi et al., 2002; Li et al., 2012). There are many factors that govern the behaviors of an expansive soil, among which the primary ones are the availability of moisture, and the amount and type of the clay-size particles in the soil (Day, 2000). Therefore, the treatment ways for expansive soils may be classified into two categories: one is the so-called mechanical and chemical stabilization (Estabragh et al., 2014) and the other is to retard moisture movement within the soil. The mechanical stabilization may include the sand cushion method (Satyanarayana, 1969), the cohesive non-swelling (CNS) layer method (Katti, 1979), the deep soil mixing (DSM) method (Madhyannapu et al., 2009; Madhyannapu and Puppala, 2014) and the synthetic reinforcement method (Al-Omari and Hamodi, 1991; Aytekin, 1997; Ikizler et al., 2008, 2009; Viswanadham et al., 2009a,b; Trouzine et al., 2012). In the chemical treatment method, lime is the most effective and economical added materials (Chen, 1988; Calik and Sadoglu, 2014). Besides, calcium chloride, fly ash and cement are also commonly used (Desai and Oza, 1977; Cokca, 2001; Al-Rawas et al., 2005; Sharma et al., 2008). The retardation of moisture movement within soils may be achieved by the coverage with natural grass cover (Zhan et al., 2007) or geomembrane and geotextile cover (Bouazza et al., 2014; Heibaum, 2014; Safari et al., 2014).

Now in China, the South-to-North Water Transfer Project (SNWTP) with three diversion routes, respectively named as the eastern, the central and the west lines, is under construction. The central diversion route is 1200 km long, of which about 180 km open channel has to pass through the expansive soil land (Ng et al., 2003). Hence, the stability of the expansive soil channel slope is particularly important for the project. The basic way to stabilize the expansive soil channel slope is to replace the expansive soils near the surface of the channel slope (about 2 m thick) with non-

* Corresponding author. Tel.: +86 15161461318; fax: +86 25 83786727.
E-mail addresses: luy@hhu.edu.cn, luyhhu@163.com (Y. Lu).

http://dx.doi.org/10.1016/j.geotexmem.2015.04.004
0266-1144/

expansive soils. However, as non-expansive soils have to be taken from areas far away from the construction site, the soil replacement way is expensive and also has some expropriation and environmental problems. Therefore, alternative ways of treating expansive soil slope have to be studied. In recent years, extensive studies have been made during the construction of the SNWTP and many other methods have been proposed for the treatment of expansive soil slopes, one of which is the use of soilbags filled with expansive soils.

Soilbags, namely geotextile bags filled with soil or soil-like materials, are commonly used in improving the bearing capacity of traditional earthworks (Matsuoka and Liu, 2006). In recent years, soilbags have been developed in some other geotechnical engineering, such as, construction of coastal protection barriers (Martinelli et al., 2011), prevention of frost heave (Li et al., 2013), reduction of mechanical vibration (Liu et al., 2014), and inclusion of retaining walls constructed in expansive soils (Wang et al., 2015). This study presents the use of soilbags to treat the expansive soil/rock channel slope. Fig. 1 shows the schematic view of the treatment for expansive soil/rock channel slope using soilbags (only the right bank is given although the left bank was treated in the same way). The expansive soils excavated in the construction field are filled into woven polypropylene bags to form soilbags, which are then arranged on the surface of the expansive soil slope to be treated. The assembly of soilbags arranged on the slope is regarded as a reinforcement layer and takes effect of restraining the expansion and contraction of expansive soils.

In the companion paper of reference (Liu et al., 2012), the reinforcement principle of soilbags and a conventional limit equilibrium equation for the stability analysis of the reinforced expansive soil slope have been presented. A series of laboratory tests were conducted and it was found that soilbags can enhance the strength and restrict the swelling deformation of the expansive soil. The permeability coefficient of the soilbag assembly ranges from 10^{-5} cm/s to 10^{-6} cm/s, which makes it possible to minimize the variation of the water contents not only in the soilbag assembly (the reinforced layer) but also in the underlying expansive soils, probably caused by the rainfall or the change of the underground water. The soilbags assembly has also a relatively high equivalent coefficient of interlayer friction because of the "interlocking effect" in the gaps between soilbags.

In this current paper, a full-scale field study of enhancing expansive soil/rock channel slope with soilbags is presented. The field test involved the construction of soilbags, the rising and falling of the channel water level as well as the natural and artificial rainfalls. During the testing period, in situ monitoring of water contents, earth pressures and lateral displacements was conducted, from which the effectiveness of enhancing expansive soil/rock channel slope with soilbags was evaluated.

2. The test site and soil profile

The test site is located in the city of Xinxiang, about 100 km North of Zhengzhou, Henan Province, China. The site is a semiarid area with an average annual rainfall ranging from 557 mm to 752 mm. About 60–70% of the annual rainfall occurs in the flood season during June and August. The average daily evaporation is about 1.3 mm and the maximum one is 5 mm.

The test site was selected on a cut slope that was prepared as part of an excavation canal (see Fig. 1). The total length of the test channel is 60 m. The slope had a mean excavation depth of 30 m, and an inclination angle of 22° (slope ratio 1:2.5) to 33.7° (slope ratio 1:1.5). The soil profile in the cut slope mainly consists of the following four layers:

(1) Brown-yellow heavy silt loam layer. It is distributed in the uppermost slope with a thickness of 2–7 m and characterized as a non-expansive soil.
(2) Gray-white marlite with a thickness of 17–18 m. The detritus minerals of the marlite are mainly composed of calcite (49–66%) and silica (10–44%); the clay minerals are mainly composed of montmorillonite and illite, accounting for 20–35% of the total mineral components. The montmorillonite and illite leads the marlite to be an expansive soil/rock with a free swelling ratio ranging from 40% to 60%. There exist many gravels and block stones as well as some invisible cracks and fissures in this layer.
(3) Brown clay rock with a depth of 7–8 m. The detritus minerals of this layer are mainly composed of calcite (9–31%) and silica (37–50%). The clay minerals account for 26–47% of the total mineral components with more montmorillonite than illite. The free swelling ratio of this layer ranges from 50% to 70%, characterizing as a medium expansivity.
(4) Brown-red sandy conglomerate distributed below the bottom of the channel. The free swelling ratio of this layer is about 50%.

The treatment of the channel slope with soilbags is mainly involved in the second and the third layers, i.e. the marlite layer and the clay rock layer. The characteristics of these two expansive soil/rock layers are given in Table 1.

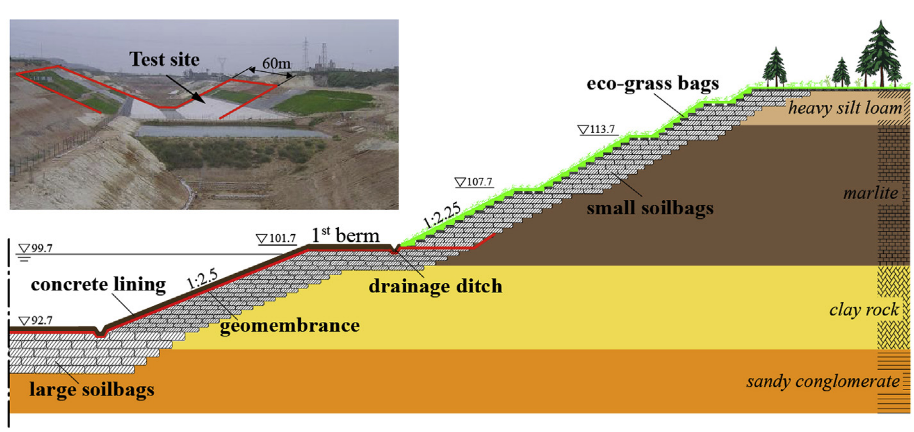

Fig. 1. Schematic view of the treatment for expansive soil/rock channel slope using soilbags.

Table 1
Characteristics of the expansive soil/rock layers.

Properties and indexes		Layers	
		Marlite	Clay rock
Physical/mechanical properties	Water content, w (%)	9.0–18.2	18.0–22.6
	Dry density, γ_d (g/cm^3)	1.71–2.13	1.66–1.81
	Optimum water content, w_{op} (%)	12.0	17.4
	Initial void ratio, e_0	0.278–0.591	0.500–0.643
	Degree of saturation, S_r (%)	73.6–99.8	91.7–99.9
	Liquid limit, LL (%)	34–57	54–63
	Plastic limit, PL (%)	16–26	21–28
	Plasticity index, PI (%)	17–37	31–38
Swelling/shrinkage indexes	Swelling pressure, S_f (kPa)	18.8–165.1	18.8–417.0
	Free swelling ratio, F_S (%)	32–69	50–67
	Linear shrinkage ratio, e_{sl} (%)	0.4–0.7	0.5–2.4
	Volumetric shrinkage ratio, e_{sv} (%)	2.4–2.7	1.5–6.6
	Shrinkage coefficient, C_S	0.03–0.06	0.21–0.36
	Cohesion, c (kPa)	13.5–40.1	11.8–35.7
	Friction angle, φ (°)	16–28	13–18

3. Construction of soilbags

As shown in Fig. 1, the soilbags were arranged on the surface of the excavated channel slope with a thickness of 2 m below the first berm and 1.5 m above the first berm. The surface of the soilbags reinforcement layer below the first berm (i.e., the water passing section) was covered with a layer of impermeable geo-membrane to control seepage and lined with a 20 cm thick concrete to reduce the channel roughness. Above the first berm, the surface of the soilbags reinforcement layer was protected with eco-grass bags.

3.1. Soilbags used

The soilbags used in the field test were made by filling the expansive soils into the woven polypropylene (PP) bags. Two different sizes of the PP bags were used: one was 57 cm × 50 cm (warp length × weft width) for the channel slope (easily handled by workers) and the other was 147 cm × 120 cm for the channel bottom (efficiently handled by machines). The properties of the PP bags are listed in Table 2. The expansive soil contained in the bags is mainly marlite excavated from the upper part of the channel slope. It has a maximum grain size of 5 cm for the small bags and 10 cm for the large bags through mechanical crushing. Approximately 25 kg and 300 kg of the expansive soils with the optimum water content of 12% are filled in one small bag and one large bag, respectively. After compaction, one small soilbag has an approximate dimension of 40 cm × 40 cm × 10 cm (length × width × height), which is formed by overlapping the bag about 7 cm in the warp direction for sewing the bag mouth; and the large one has an approximate dimension of 100 cm × 100 cm × 20 cm with the overlap length of 27 cm in the warp direction.

Table 2
Properties of the PP bags.

Items	Small size	Large size
Warp length × weft width (cm)	57 × 50	147 × 120
Mass per square meter (g/m^2)	≥100	≥150
Warp tensile strength (kN/m)	≥25	≥30
Weft tensile strength (kN/m)	≥16.2	≥30
Warp and weft elongation (%)	≤25	≤25
Color	Black (higher capability of anti-ultraviolet rays)	

3.2. Placement and compaction of soilbags

Fig. 2 shows the placement and compaction of soilbags in the test field. First, five layers of large soilbags with a total thickness of 1 m were placed on the bottom of the channel by using a crane. The interspaces between the soilbags in each layer were filled with the same expansive soils as contained in the bags. The adjacent two layers should be arranged in a staggered way. Each layer was compacted two or three passes with vibratory rollers, as shown in Fig. 2(a). The compaction degree of the soil contained in the bags was greater than 85%. Then, small soilbags were manually arranged along the channel slope and compacted with small plate vibrators layer by layer, as shown in Fig. 2(b). The compaction degree of the soil contained in the small bags is the same as that in the large bags. The horizontal width of the soilbags layer is 5.4 m (the thickness 2 m) below the first berm and 2.7–3.7 m (the thickness 1.5 m) above the first berm. After the construction of the soilbags, the concrete lining and a layer of eco-grass bags were placed on the surface of the soilbags below the first berm and above the first berm, respectively, as shown in Fig. 2(c) and (d).

4. Instrumentation and observation

4.1. Instrumentation layout

Fig. 3 shows the instrumentation layout on the channel slope. The instruments included theta moisture probes (abbreviated as MP), earth pressure cells (PC) and inclinometer tubes (IT). There were two rows of MP for monitoring water contents that were installed into the slope below and above the first berm, respectively. Each row has one MP inside the soilbags layer (about 1 m deep, denoted as B1.0) and three MPs inside the expansive soil slope with an installed depth of 0.5 m, 1.5 m and 2.5 m (denoted as S0.5, S1.5 and S2.5), respectively. The moisture probes at each row were spaced 1.5 m apart, as shown in Fig. 3(b). In total, 8 moisture probes were installed for water content measurements. After installing each of the moisture probes, the installation holes were backfilled with moist soil, which was compacted to a dry density close to the in-situ dry density.

There were two groups of PCs installed in the interface between the soilbags layer and the excavated expansive soil/rock slope. In each group, three PCs with 1.5 m space apart were pasted onto a U-shaped steel that was anchored into the slope, as shown in Fig. 4. One PC was contacted with the soilbags layer that was used to

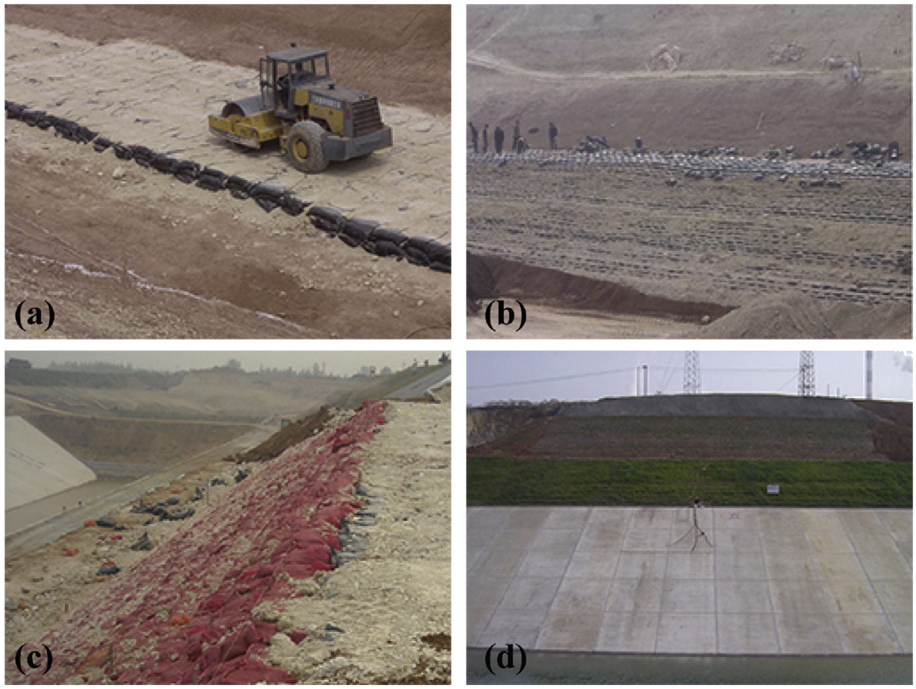

Fig. 2. Photos of soilbags construction: (a) Compaction of large soilbags on the channel bottom; (b) Construction of soilbags on the channel slope; (c) Eco-grass bags above the first berm; (d) Construction completion.

measure the overburden pressure; the other two PCs on the opposite face of the U-shaped steel were intended to measure the swelling pressure of the expansive soil/rock as the U-shaped steel was anchored into the slope. The U-shaped steel was parallelly close to the row of the MPs so that the connection wires of both the MPs and the PCs can be drawn out through an outlet tube, as shown in Fig. 3(a). The data from the MPs and the PCs were collected using a data logger.

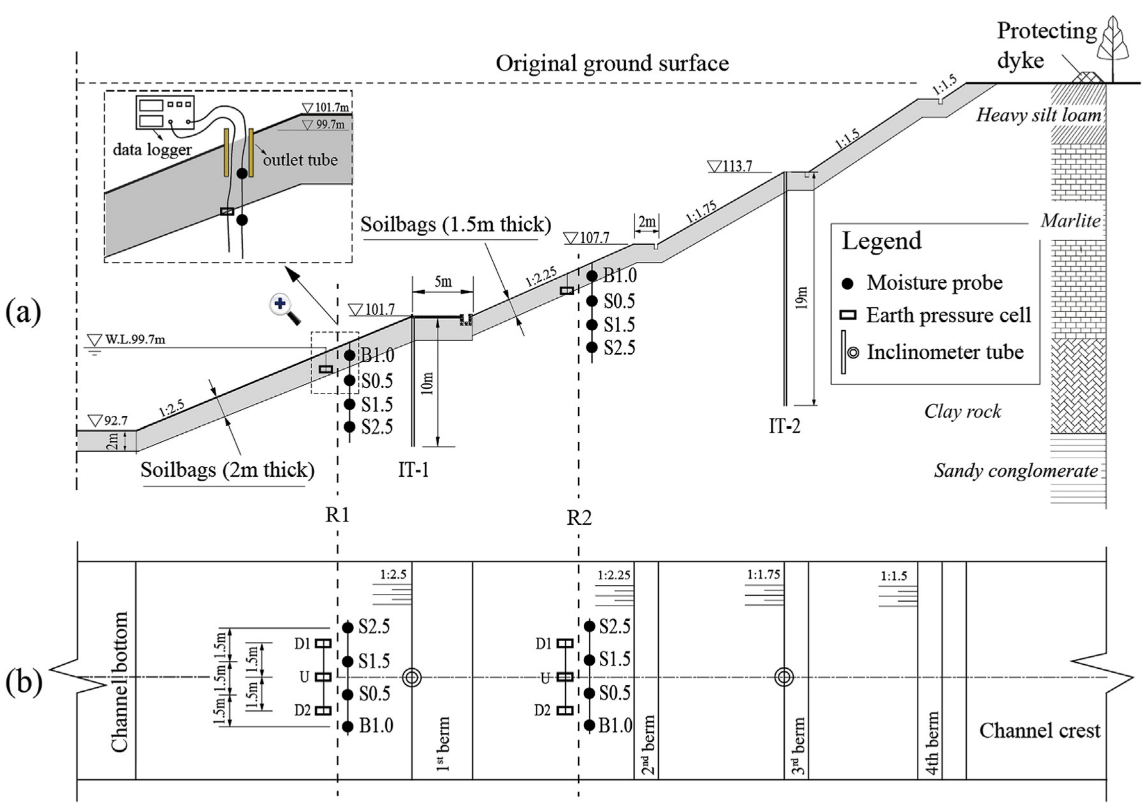

Fig. 3. Instrumentation layout on the channel slope: (a) Cross section; (b) Vertical view.

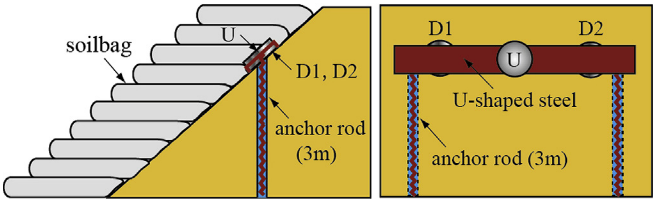

Fig. 4. Schematic layout of earth pressure cell (PC).

Moreover, as illustrated in Fig. 3, two 10 m and 19 m long inclinometer tubes were installed into the first berm and the third berm, respectively, which were used to measure the lateral displacements of the tested expansive soil/rock slope.

4.2. Observation record

The observation record period in the test site lasted for more than two years (i.e., from January, 2008 to May, 2010), during which time it experienced the construction of the soilbags, the rising and falling of the channel water level as well as the natural and artificial rainfalls.

The soilbags below the first berm were constructed from April 27 to May 30, 2008, whose surfaces were lined with concrete from June 2 to 12, 2008. The soilbags between the first and the second berms were constructed from June 17 to 27, 2008. The construction of soilbags above the 2nd berm was from Aug. 5 to Sept. 3, 2008.

Two rising and falling processes of the channel water level were simulated: 1) rising from EL.92.7 m to EL.94.7 m during Oct. 23–25, 2008 and further to EL.99.7 m during Dec. 3–8, 2008; 2) falling from EL.99.7 m to EL.97.7 m during April 5–9, 2009 and further to EL.92.7 m during Nov. 29 to Dec. 22, 2009.

During the construction period of the soilbags and the concrete lining, the test site experienced four relatively larger rainfalls with a total precipitation of 15–30 mm each time. After the construction, one heavy rainfall with a total precipitation as high as 90 mm was recorded on July 14, 2008, and a 22 mm rainfall was recorded on Aug. 13, 2008. During the period of Aug. 13, 2008 to Jan. 26, 2009, no natural precipitation occurred and the test site was subjected to a continuous drought. To further investigate the effect of the soilbags layer, the artificial rainfalls with a mean intensity of about 50 mm/d were simulated during Mar. 9–20, 2009. After then, some subsequent small natural rainfalls were observed.

5. Results and discussions

5.1. Water content

Fig. 5 shows the changes of volumetric water contents inside the expansive soil/rock slope from April to June, 2008. During this period, the soilbags and the concrete lining below the first berm were under construction, and the testing site experienced four

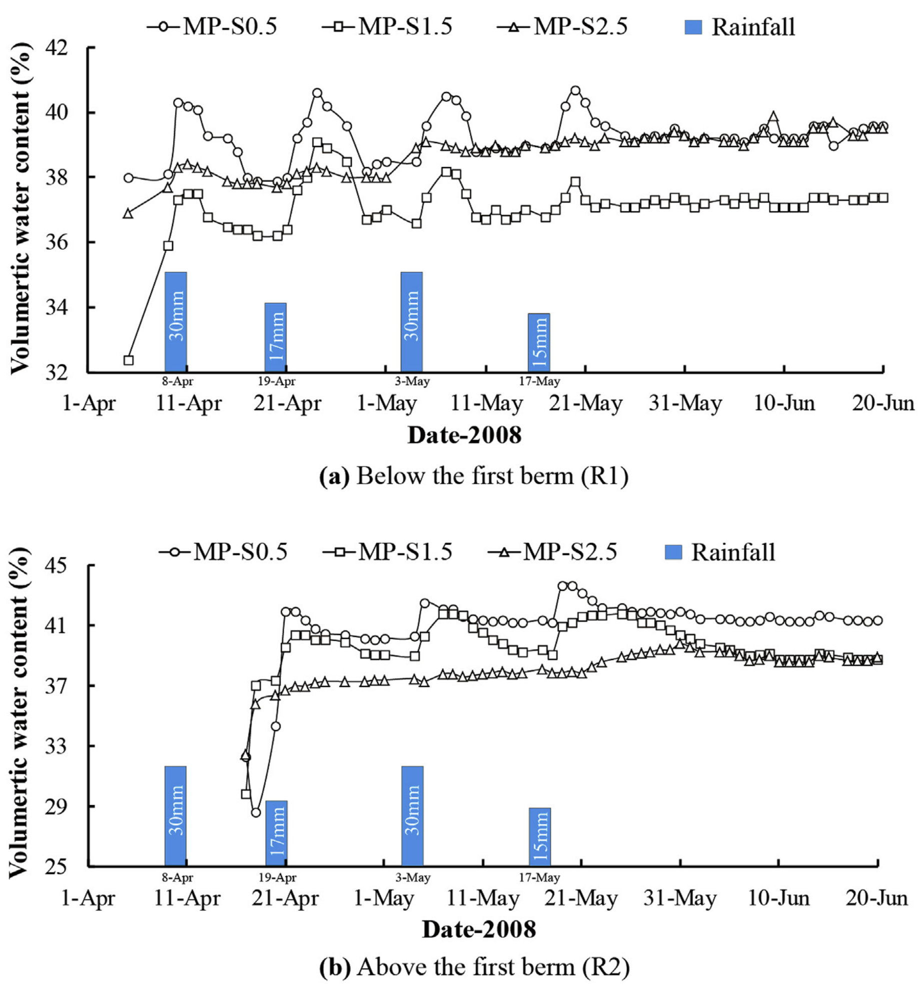

Fig. 5. Changes of volumetric water contents during the construction: (a) Below the first berm (R1); (b) Above the first berm (R2).

rainfalls. It was observed that the rainfalls caused a significant increase and then a prompt decrease in the volumetric water contents of the expansive soil/rock slope within the depth of 1.5 m (measured by the MP-S0.5 and MP-S1.5). However, the increase in the volumetric water content below 1.5 m was not so significant, as measured by the MP-S2.5. Moreover, the delayed response of the volumetric water content to the rainfalls was observed. In another test conducted by Zhan et al. (2007) in SNWTP, a significant increase of the water content was also observed within the top 1.5 m of the bare expansive soil slope, which may be due to the some deep, extended open cracks at the upper part of the slope. Before soilbags were placed, the expansive soil/rock slope within a depth of approximate 1.5 m, the so-called atmospheric influence region, is influenced significantly by rainfalls.

During the entire monitoring period, the changes of volumetric water contents inside the expansive soil/rock slope below and above the first berm are given in Fig. 6(a) and (b), respectively. The entire monitoring period is divided into four stages, denoting by ①–④, in which stage ① corresponds to the construction period as shown in Fig. 5. It can be seen from Fig. 6 that after the construction period (i.e. stages ②–④), the changes of the volumetric water contents are pronounced inside the soilbags-reinforced layers in response to the fluctuation of the channel water level as well as the rainfalls, as measured by MP-B1.0; however, they are not remarkable (almost steady) inside the expansive soil/rock slope, as measured by the MP-S0.5, MP-S1.5 and MP-S2.5. It is indicated that solibags-reinforced layers can minimize the infiltration of rainfalls into the underlying expansive soil/rock slope, acting as a protective layer.

As shown in Fig. 6(a), the change of the volumetric water content inside the soilbags layer below the first berm can be explained as follows: a) during stage ②, it was caused by the rainfall infiltration from the unlined drainage ditch on the inner side of the first berm; b) at the begin of stage ③, the rapid increase of the water content was due to the entrance of the channel water from the outlet tube of the connecting wires when the channel water level increased up to EL.99.7 m; c) during stage ④, the decrease in the water content resulted from the subsequent drawdown of the channel water level from EL.99.7 m to EL.97.7 m, and then the water content tended to a stable value. The data missing after July 26, 2009 was due to the damage of the MP-B1.0. As the soilbag assembly has the permeability coefficient of 10^{-5} to 10^{-6} m/s (the horizontal permeability coefficient is nearly 10 times higher than the vertical one), much larger than that of the saturated expansive soil (about 10^{-8} m/s), the soilbag assembly can be regarded as a semi-permeable material, and any water penetrating into it may drain away quickly. Therefore, in this field test, the more pronounced change of the volumetric water content inside the soilbags layer is attributed to the relatively higher permeability of the soilbags layer compared to the underlying expansive soil/rock due to the existence of gaps and contact surfaces between soilbags.

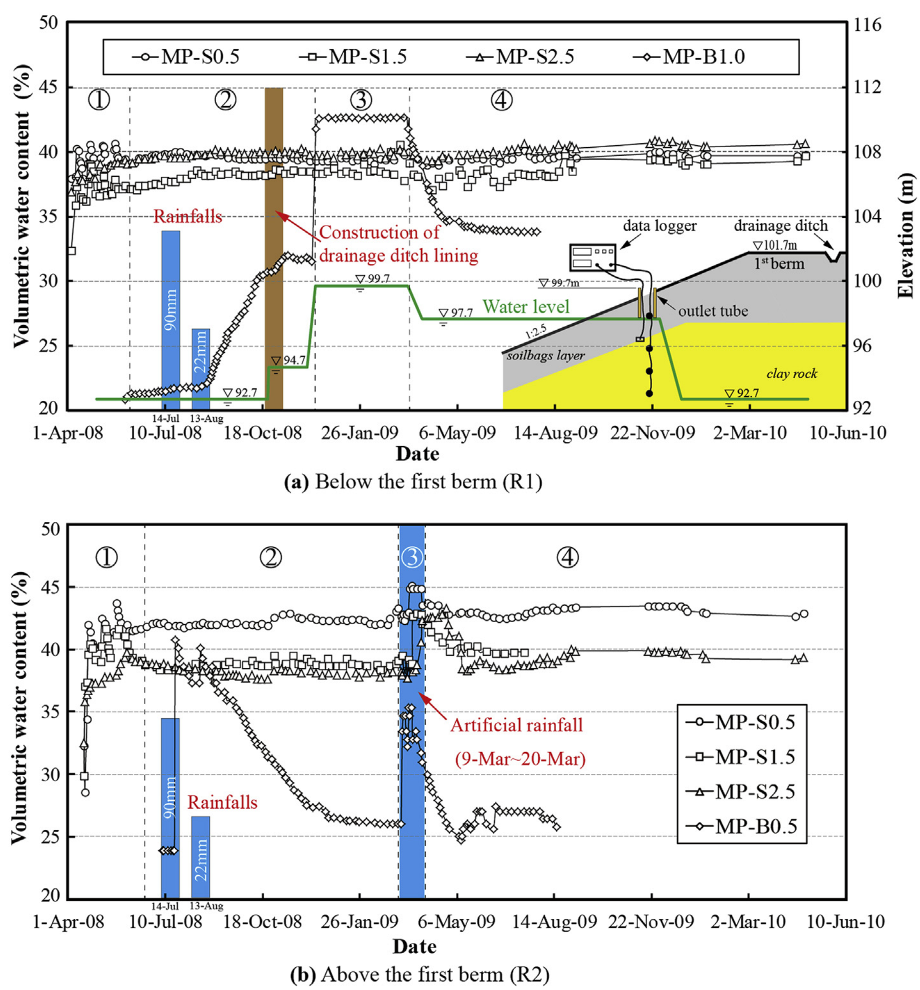

Fig. 6. Changes of volumetric water contents during the entire monitoring period: (a) Below the first berm (R1); (b) Above the first berm (R2).

As the slope above the first berm is protected with permeable eco-soilbags, the changes of the volumetric water contents in response to the rainfalls and evaporation above the first berm are relatively more significant than those below the first berm, especially inside the soilbags layer. During stage ②, the slope experienced one heavy rainfall with a total precipitation as high as 90 mm (July 14, 2008), Fig. 6(b) shows that the volumetric water content inside the soilbags layer increased rapidly from 24% to 41%, then decreased to 37.5% due to the evaporation and infiltration, and again increased to 40% due to the 22 mm rainfall on Aug. 13, 2008. From Aug. 13, 2008 to Jan. 26, 2009, the continuous drought in the test site caused the decrease of the volumetric water content inside the soilbags layer from 40% to 26%, but the water contents inside the expansive soil/rock slope remained nearly steady, indicating the good water retention ability of the soilbag assembly layer for the underlying expensive soil/rock slope in an arid climate condition. During Mar. 9 to Mar. 20, 2009, the artificial rainfalls with a mean intensity of about 50 mm/d were simulated to further investigate the effect of the soilbags layer. It can be seen from Fig. 6(b) that during the artificial rainfalls (stage ③), the changes of the volumetric water content inside the soilbags layer are more significant than those inside the underlying expansive soil/rock slope, as measured by MP-B0.5, MP-S0.5, MP-S1.5 and MP-S2.5. It was attributed to the relatively high permeability of the soilbags assembly, especially along the horizontal inter-layers. Thus, the soilbag assembly has an effect of reducing the infiltration of rainfalls into the underlying expansive soil/rock slope. After the artificial rainfalls (stage ④), the water content inside the soilbags layer decreased gradually and tended to a stable value although there was some slight fluctuation due to some small natural rainfalls. The subsequent missing data of MP-B0.5 and MP-S1.5 were due to the damage of the sensors.

5.2. Earth pressure

Fig. 7 shows the measured earth pressures inside the soilbags layer and the underlying expansive soil/rock slope. As stated previously, the PC-U on the upper side of the U-shaped steel was used to measure the overburden pressure of the soilbags layer, while the PC-D1 and PC-D2 on the opposite face of the U-shaped steel were designed to approximately measure the swelling pressures of the underlying expansive soil/rocks. The changes of the measured earth pressures may also be analyzed in four stages, in which stage ① refers to the period before the completion of the soilbags layer construction. Before the construction of the soilbags layer, no overburden pressure was measured by the PC-U, and the maximum swelling pressures due to rainfalls, measured by the PC-D1 and PC-D2, were averagely about 26.3 kPa and 14.5 kPa below and above the first berm, respectively. During the construction of the soilbags layer, the measurement values of the three PCs increased greatly due to the influence of the construction machines and compaction, as shown in Fig. 7(c) and (d). After the completion of the soilbags layer construction, the values measured by the PCs decreased gradually. During stage ②, as shown in Fig. 7(a) and (b), the values measured by the PC-U tended to the overburden pressures of 30 kPa of the 2 m thick soilbags layer below the first berm and 22.5 kPa of the 1.5 m thick soilbags layer above the first berm. The average values measured by the PC-D1 and PC-D2 below and above the first berm were 54.2 kPa and 28.4 kPa, respectively, nearly the swelling pressures of clay rock and marlite at the moisture and density of the site measured by Yangtze River Scientific Research Institute (2010). Below the first berm, the channel water level increased up to 99.7 m and the water flowed into the outlet tube of the connecting wires during stage ③. The wetting-induced weight increase of the soilbags led to the increase of the overburden pressure by about 8.7 kPa, as shown in Fig. 7(a). Above the first berm, an artificial rainfall was produced, resulting in the increases of the overburden pressure and the swelling pressure during stage ③, as shown in Fig. 7(b). However, the increase of the overburden pressure induced by the weight increase of the soilbags is more prominent than the increase of the swelling pressure of the expansive soil/rock caused by the limited infiltration of the artificial rainfall. During stage ④, the measurement values of the PCs approached to those as measured at the end of stage ②, although there were some small variations caused by natural rainfalls.

As aforementioned, the measurement by the PC-D1 and PC-D2 is approximately the swelling pressure in the underlying expansive soil/rock slope. The comparison of Fig. 6 with Fig. 7 indicates that the swelling pressure is inter-linked with the water content measured nearby (MP-S0.5) after the completion of the soilbags layer construction. During that period, as a result of the protection of the soilbags layer, the changes of both the measured water content and the swelling pressure are small in the underlying expansive soil/rock slope. During stage ③ above the first berm, the increase of the water content caused by the infiltration of the artificial rainfall leads to the increase in the swelling pressure. However, it is noticed that this inter-linked relationship is not obvious in the soilbags-reinforced layer because the swelling deformation of expansive soils is restrained by the bags and the soilbags layer is equivalent to a non-expansive layer. The reduced swelling of the expansive soil was attributed to the tensile forces T along the perimeters of the bags, which developed due to the extension of the bag under the heaving deformation action occurring during the wetting process, which is also validated in a model test by Wang et al. (2015).

5.3. Lateral displacement

Fig. 8 gives the distributions of the lateral displacements along the slope depth, measured by IT-1 and IT-2 that were installed in the outer side of the first berm and the third berm, respectively. The positive value denotes the lateral displacement toward the channel. The maximum lateral displacements measured by IT-1 and IT-2 are 25.5 mm and 15 mm, respectively. The relatively large lateral displacements measured by IT-1 are within the soilbags layer (above EL.99.7 m), and those measured by IT-2 are within the slope depth between EL.104 m and EL.113.7 m. In Fig. 8(a), the smaller lateral displacements at the topmost than those at the subsequent shallow depth (EL.101.2 m) may result from the restraint of the concrete lining. The similar phenomena observed by IT-2 in May 8 and July 25, 2009, as shown in Fig. 8(b), may be attributed to the shrinkage of the expansive soils contained in the surface soilbags.

Fig. 9 shows the evolutions of the lateral displacements measured at some typical elevations. It is seen from Fig. 9(a) that the evolutions of the lateral displacements measured at the three different elevations are almost the same, but the magnitudes at EL.101.2 m are much greater than those at EL.99.7 m and EL.96.7 m. Before November, 2008, the increase in the lateral displacements (a–b in Fig. 9(a)) was mainly caused by the construction machines running at the first berm, the rainfall infiltration from the slope surface and the unlined drainage ditch at the inner side of the first berm; impounding of the channel water up to EL.99.7 m caused a slight decrease (about 4 mm, c–d in Fig. 9(a)) in the lateral displacement (backward the slope); Subsequently, as the outlet tube of the connecting wires at EL.99.7 m was not well sealed, the channel water entered into the soilbags layer from the outlet tube. As a result, the interface friction between the wetting soilbags decreased and thereby the lateral displacement increased (e–f in Fig. 9(a)). When the channel water level fell from EL.99.7 m to

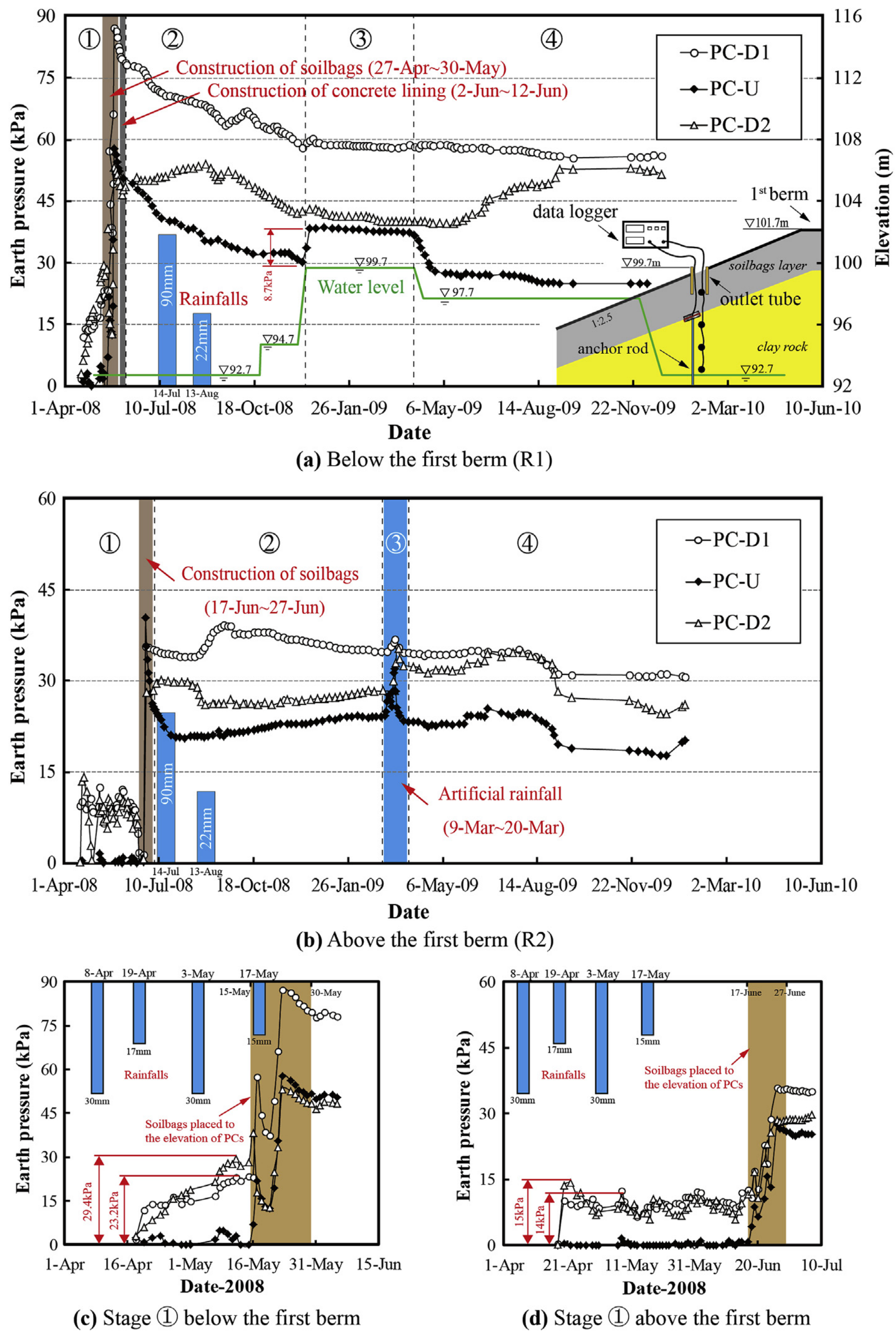

Fig. 7. Changes of earth pressures measured by PCs: (a) Below the first berm (R1); (b) Above the first berm (R2); (c) Stage ① below the first berm; (d) Stage ① above the first berm.

EL.97.7 m, the water inside the soilbags layer drained gradually and the lateral displacement recovered under the action of the channel water pressure at EL.97.7 m and tended to a relative stable value (f–g–h in Fig. 9(a)).

The soilbags above the second berm were constructed during August 5 and September 3, 2008. Before August 5, 2008, the lateral displacements measured by IT-2 were mainly caused by the excavation unloading and the rainfall infiltration into the bare expansive soil/rock slope. After the completion of the soilbags construction, the lateral displacements measured by IT-2 at the four different elevations changed slightly even during the artificial rainfalls, as shown in Fig. 9(b). The effectiveness of the soilbags on the stability of the expansive soil/rock slope was thus indicated.

6. Conclusions

A full-scale field study of treatment for expansive soil/rock channel slope with soilbags was conducted to investigate the influence of soilbags construction, variation of channel water level and rainfalls on the changes of water content, earth pressure and lateral displacement in the soilbags layer and the underlying expansive soil/rock slope. Based on the field monitored results, the following conclusions can be obtained:

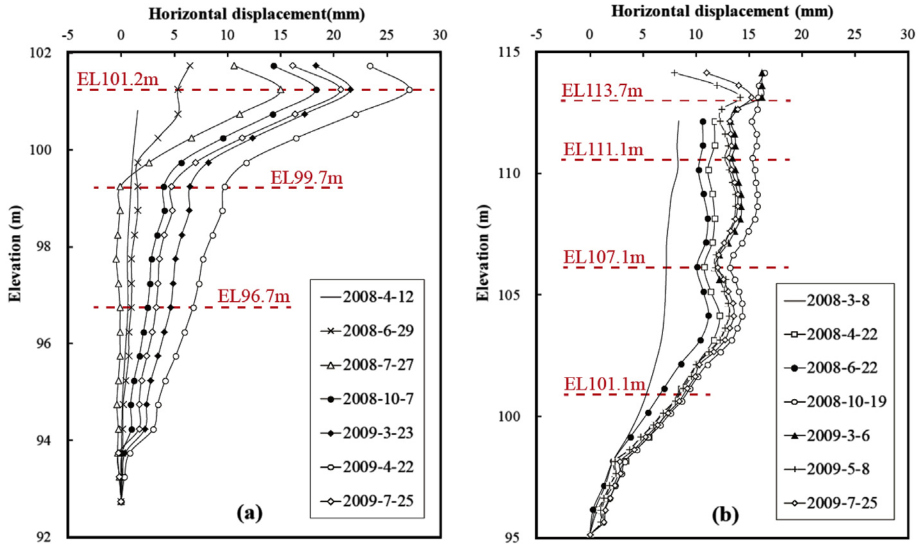

Fig. 8. Distributions of lateral displacements of the slope along the depth: (a) Measured by IT-1; (b) Measured by IT-2.

(1) The water content in the bare expansive soil/rock channel slope was significantly affected by rainfalls and evaporation. After the completion of soilbags construction, the water content inside the soilbags layer exhibited certain changes with the variation of the channel water level and rainfalls, but it was almost unchanged inside the underlying expansive soil/rock slope. These results indicated that the soilbags layer can effectively retard the moisture movement into the underlying expansive soil/rock slope.

(2) The earth pressures measured in the interface between the soilbags layer and the expansive soil/rock slope were greatly affected by the construction of soilbags. After the completion

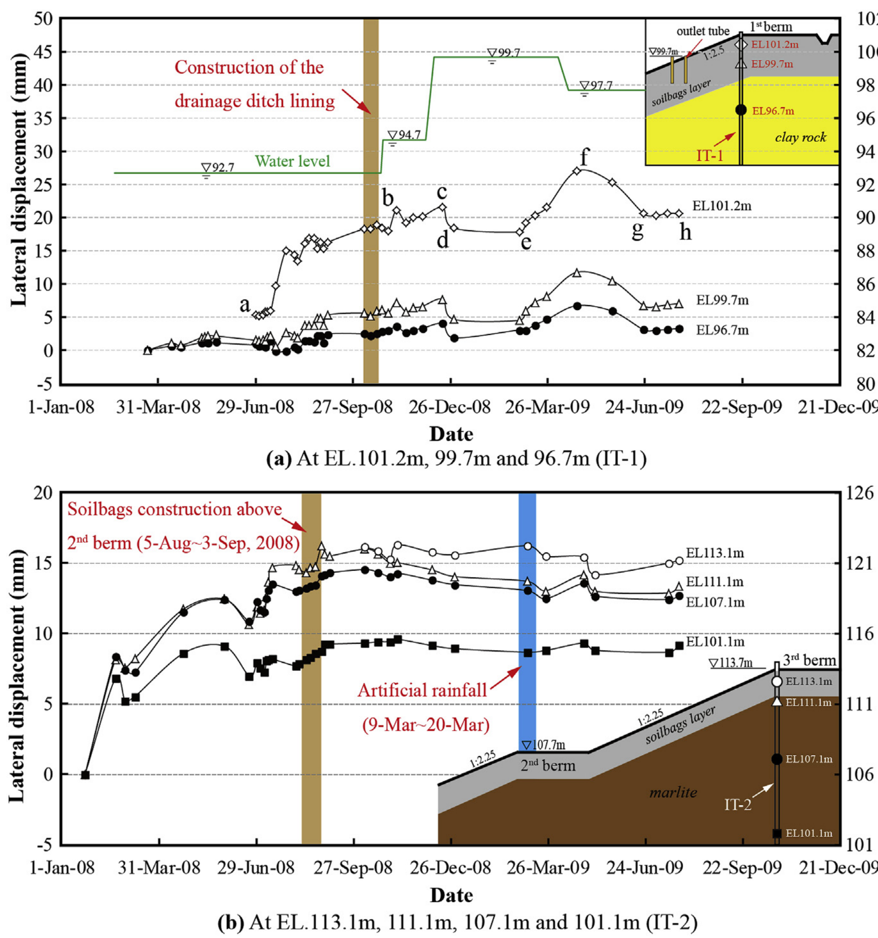

Fig. 9. Evolutions of lateral displacements of the slope at some typical elevations: (a) At EL.101.2 m, 99.7 m and 96.7 m (IT-1); (b) At EL.113.1 m, 111.1 m, 107.1 m and 101.1 m (IT-2).

of the soilbags layer construction, the earth pressures measured inside the expansive soil/rock slope nearly tended to the swelling pressures of the expansive soil/rock and those measured under the soilbags layer were close to the overburden pressures of the soilbags layer. This measurement suggests that the soilbags layer acts as a non swelling reinforcement layer, and presses the underlying expansive soil/rock slope.

(3) The lateral displacements of the expansive soil/rock channel slope were mainly caused by the slope excavation unloading and the soilbags construction. After the completion of soilbags construction, they changed slightly even though the channel slope was subjected to rainfalls.

Acknowledgments

The authors would like to acknowledge the constructive suggestion and the great help from Yisen Wang. This work was supported by the National Natural Science Foundation of China (51379066) and the Key Projects in the National Science and Technology Pillar Program during the 11th 5-year Plan Period of PR China (Grant No. 2006 BAB04A10). It was also a part of work in the project funded by the Priority Academic Program Development of Jiangsu Higher Education Institutions (PAPD) (Grant No. YS11001). These supports are gratefully acknowledged. The authors also appreciate the assessors' excellent comments and constructive suggestions to the study.

References

Al-Omari, R.R., Hamodi, F.J., 1991. Swelling resistant geogrid – a new approach for the treatment of expansive soils. Geotext. Geomembr. 10 (4), 295–317.
Aytekin, M., 1997. Numerical modeling of EPS geofoam used with swelling soil. Geotext. Geomembr. 15 (1), 133–146.
Al-Rawas, A.A., Hago, A.W., Al-Sarmi, H., 2005. Effect of lime, cement and Sarooj (artificial pozzolan) on the swelling potential of an expansive soil from Oman. Build. Environ. 40 (5), 681–687.
Bouazza, A., Singh, R.M., Rowe, R.K., Gassner, F., 2014. Heat and moisture migration in a geomembrane–GCL composite liner subjected to high temperatures and low vertical stresses. Geotext. Geomembr. 42 (5), 555–563.
Chen, F.H., 1988. Foundation on Expansive Soils. Elsevier, Amsterdam, Netherlands.
Cokca, E., 2001. Use of class C fly ashes for the stabilization of an expansive soil. J. Geotech. Geoenviron. Eng. 127 (7), 568–573.
Calik, U., Sadoglu, E., 2014. Classification, shear strength, and durability of expansive clayey soil stabilized with lime and perlite. Nat. Hazards 71 (3), 1289–1303.
Desai, I.D., Oza, B.N., 1977. Influence of anhydrous calcium chloride on the shear strength of expansive soil. In: Proc. of the 1st National Symposium on Expansive Soils, HBTI-Kanpur, India, pp. 4-1–4-5.
Dif, A.E., Bluemel, W.F., 1991. Expansive soils under cyclic drying and wetting. Geotech. Test. J. 14 (1), 96–102.
Day, R.W., 2000. Geotechnical Engineer's Portable Handbook. McGraw-Hill, New York.
Estabragh, A.R., Rafatjo, H., Javadi, A.A., 2014. Treatment of an expansive soil by mechanical and chemical techniques. Geosynth. Int. 21 (3), 233–243.
Heibaum, M., 2014. Geosynthetics for waterways and flood protection structures – controlling the interaction of water and soil. Geotext. Geomembr. 42 (4), 374–393.
Ikizler, S.B., Aytekin, M., Nas, E., 2008. Laboratory study of expanded polystyrene (EPS) geofoam used with expansive soils. Geotext. Geomembr. 26 (2), 189–195.
Ikizler, S.B., Aytekin, M., Vekli, M., 2009. Reductions in swelling pressure of expansive soil stabilized using EPS geofoam and sand. Geosynth. Int. 16 (3), 216–221.
Ito, M., Azam, S., 2010. Determination of swelling and shrinkage properties of undisturbed expansive soils. Geotech. Geol. Eng. 28, 413–422.
Katti, R.K., 1979. Search for solutions to problems in black cotton soils. Indian Geotech. J. 9 (1), 1–80.
Liu, S.H., Bai, F.Q., Wang, Y.S., Wang, S., Li, Z., 2012. Treatment for expansive soil channel slope with soilbags. J. Aerosp. Eng. 26 (4), 657–666.
Li, X.W., Wang, Y., Yu, J.W., Wang, Y.L., 2012. Unsaturated expansive soil fissure characteristics combined with engineering behaviors. J. Cent. South Univ. 19, 3564–3571.
Li, Z., Liu, S.H., Wang, L.J., Zhang, C.C., 2013. Experimental study on the effect of frost heave prevention using soilbags. Cold Regions Sci. Technol. 85, 109–116.
Liu, S.H., Gao, J.J., Wang, Y.Q., Weng, L.P., 2014. Experimental study on vibration reduction by using soilbags. Geotext. Geomembr. 42 (1), 52–62.
Morris, P.H., Graham, J., Williams, D.J., 1992. Cracking in drying soils. Can. Geotech. J. 29 (2), 263–277.
Matsuoka, H., Liu, S.H., 2006. A New Earth Reinforcement Method Using Soilbags. Taylor & Francis/Balkema, The Netherlands.
Madhyannapu, R.S., Puppala, A.J., Nazarian, S., Yuan, D., 2009. Quality assessment and quality control of deep soil mixing construction for stabilizing expansive subsoils. J. Geotech. Geoenviron. Eng. 136 (1), 119–128.
Martinelli, M., Zanuttigh, B., Nigris, N.D., Preti, M., 2011. Sand bag barriers for coastal protection along the Emilia Romagna littoral, Northern Adriatic Sea, Italy. Geotext. Geomembr. 29 (4), 370–380.
Madhyannapu, R.S., Puppala, A.J., 2014. Design and construction guidelines for deep soil mixing to stabilize expansive soils. J. Geotech. Geoenviron. Eng. 140 (9), 1–15.
Ng, C.W.W., Zhan, L.T., Bao, C.G., Fredlund, D.G., Gong, B.W., 2003. Performance of an unsaturated expansive soil slope subjected to artificial rainfall infiltration. Geotechnique 53 (2), 143–157.
Satyanarayana, B., 1969. Behavior of expansive soil treated or cushioned with sand. In: Proceedings of 2nd International Conference on Expansive Soils, Texas, pp. 308–316.
Shi, B., Jiang, H., Liu, Z., Fang, H.Y., 2002. Engineering geological characteristics of expansive soils in China. Eng. Geol. 67 (1), 63–71.
Sharma, R.S., Phanikumar, B.R., Rao, B.V., 2008. Engineering behavior of a remolded expansive clay blended with lime, calcium chloride, and rice-husk ash. J. Mater. Civ. Eng. 20 (8), 509–515.
Safari, E., Jalili Ghazizade, M., Abduli, M.A., Gatmiri, B., 2014. Variation of crack intensity factor in three compacted clay liners exposed to annual cycle of atmospheric conditions with and without geotextile cover. Waste Manag. 34, 1408–1415.
Trouzine, H., Bekhiti, M., Asroun, A., 2012. Effects of scrap tyre rubber fibre on swelling behaviour of two clayey soils in Algeria. Geosynth. Int. 19 (2), 124–132.
Viswanadham, B.V.S., Phanikumar, B.R., Mukherjee, R.V., 2009a. Swelling behaviour of a geofiber-reinforced expansive soil. Geotext. Geomembr. 27 (1), 73–76.
Viswanadham, B.V.S., Phanikumar, B.R., Mukherjee, R.V., 2009b. Effect of polypropylene tape fibre reinforcement on swelling behaviour of an expansive soil. Geosynth. Int. 16 (5), 393–401.
Wang, L.J., Liu, S.H., Zhou, B., 2015. Experimental study on the inclusion of soilbags in retaining walls constructed in expansive soils. Geotext. Geomembr. 43 (1), 89–96.
Yangtze River Scientific Research Institute, 2010. Research Report on Failure Mechanism and Treatment Technology for Expansive Soil Channel Slope (Wuhan, China).
Zhan, T.L., Ng, C.W.W., Fredlund, D.G., 2007. Field study of rainfall infiltration into a grassed unsaturated expansive soil slope. Can. Geotech. J. 44 (4), 392–408.
Zemenu, G., Martine, A., Roger, C., 2009. Analysis of the behaviour of a natural expansive soil under cyclic drying and wetting. Bull. Eng. Geol. Environ. 68 (3), 421–436.